



International Journal OF Engineering Sciences & Management Research

ENHANCING THE PERFORMANCE OF UBAKALA CLAY FOR USE AS DRILLING MUD

IgweI.K.¹, ObijiakuJ.C.*² & OgahA.O.³

^{1&2}Department of Chemical Engineering, Federal University of Technology, P.M.B 1526, Owerri, Nigeria.

³Department of Food Science and Technology, Federal University, Ndufu-Alike, Ikwo, Ebonyi State, Nigeria.

Key Words: Ubakala clay, sodium carbonate, concentration, viscosity, speed of agitation, time, kinetics, statistical models, Gaussian

ABSTRACT

Drilling mud. A sample of Nigerian clay (Ubakala clay) was used for the project. The clay sample was collected in a raw state, processed and experiments conducted on viscosity which is a very important property of drilling mud. Various concentrations of sodium carbonate were mixed with the clay sample and experiments were conducted to determine the viscosities of the control and the clay-sodium carbonate mixture at periodic time intervals and various speeds of agitation. Response Surface Methodology was used, and with the aid of a MATLAB programming, to study the data obtained from the experiment. The results showed that sodium carbonate concentration, speed of agitation and their various interactions terms and quadratic terms are the significant variables in the statistical model with time being the least significant of the three factors studied. Furthermore, on analysis of the kinetics of the process, a Gaussian model, having the highest values of R^2 (50% for Gaussian model, and 25% each for Exponential and Exponential Power models) and the lines of best fit, effectively describes the kinetics of the process and the viscosity of the clay samples in relation to time, concentration of sodium carbonate and speed of agitation. Further work on the Gaussian model gave rise to a new model that can be used to determine the values of the kinetic constants. This new model showed that a speed of agitation between 300rpm and 600rpm gave the best result for the process.

INTRODUCTION

Nigeria's economy is largely based on its oil resources and she is the largest oil producer in sub-Saharan Africa. In view of the fact that hydrocarbon and water beneath the ground could only be exploited through drilling wells, the petroleum industry especially has continued to make increasing use of clay which is the main constituent of drilling fluids.

Research over the past several years has clearly shown that drilling activities in the petroleum and ground-water development industries in Nigeria have consumed, and are still consuming, large amounts of clays for drilling muds, all of which are imported despite the presence of large reserves of clay in Nigeria (Omole et al., 1989). This is because Nigerian clays have poor viscosity due to high calcium content unlike the imported clays that are rich in sodium. Prior to the government's initiative to develop local content, the cost of importation of bentonite for drilling activities in Nigeria was running into millions of dollar annually which has been detrimental to the economy of the country considering that about 5 to 15% of the cost of drilling a well which ranges between \$1 million to \$100 million accounts for drilling fluids (Ben Bloys et al., 1994) Therefore, it is imperative to locally outsource these clay materials in order to conserve foreign exchange, create employment and to enhance Nigerian content development in the drilling component of oil and gas industry.

It was reported by Emofurieta (2010) that Nigeria bentonite proven reserve has risen above four billion metric tons. Thus, its abundant reserve cannot be ignored because of increased revenue it will generate when fully exploited and more so as means of developing economy of the country through creation of more industries which will consequently lead to local skill transfer and man power development.

The selection of the most suitable mud type and mud properties, and the efficient engineering support whilst drilling will help to ensure a safe and successful operation. Any problem where the mud fails to meet its requirements can not only prove extremely costly in materials and time, but also jeopardize the successful completion of the well and may even result in major problems such as kicks or blowouts.



International Journal OF Engineering Sciences & Management Research

Hence it is necessary to critically examine the suitability of Nigerian clays in regards to their rheological properties.

Raw materials used for the mud making are usually selected clays and are judged by their behaviour in water (Nestle, 1944). Their suitability is determined by various criteria, among which are the volumetric yield of given clay, soluble impurities, abrasives content, and filtration characteristics. The raw material which meets most of these requirements for drilling is the bentonite clay. Bentonite is formed by the weathering of volcanic ash. The weathering process, by which the clay minerals are formed from the parent minerals are complex but the main factors are climate, topography, vegetation, and time of exposure (Jackson, 1957).

Bentonite was named after Fort Benton (Wyoming, USA), the locality where it was first found. In addition to montmorillonite, bentonite may also contain feldspar, biotite, kaolinite, illite, cristobalite, pyroxene, zircon, and crystalline quartz (Parkes, 1982). By extension, the term bentonite is applied commercially to any plastic, colloidal, and swelling clay regardless of its geological origin. Such clays are ordinarily composed largely of minerals of the montmorillonite group.

Research performed in the early 90's by the Bureau of Mines of the U.S.A, showed that the sum of bentonite deposits in the world was about 1.36 billion tons, and the U.S.A. has more than 50.0% of the total (Amorin et al., 2007).

The need to search for local alternatives to bentonite and other additives, which are used in the drilling of oil and gas, is imperative and timely. Apart from the significant infrastructural development in the area of mining (Falode et al., 2007), the industry could be developed to the extent of exporting locally produced bentonite out of the country hence increase the country's revenue.

This research work focuses mainly on enhancing the performance of Nigerian clay deposits for use as drilling mud.

METHOD

Experimentation

Processing the Clay Samples

The collected clay sample is sun-dried to remove moisture and then pounded with the aid of a mortar and pestle to reduce the particle size and increase the surface area. The pounded clay sample is then put in a furnace for further drying to remove the possible moisture content in sample. After drying, the sample is taken to mill for further grinding to get the desired particle size. A hammer mill is mounted vertically and is designed to have two funnels. The upper funnel serves as the clay sample inlet while the bottom one serves as the clay sample outlet. The mill has a hammer at the centre which is driven by an electric motor part of the mill. The function of the hammer is to continuously reduce the particles of the clay to obtain the desired size. Below the hammer is a sieve with mesh. The mesh is changeable and the mesh size used determines the size of the clay particle to be obtained. After passing through the mill, the clay gotten is packaged for experiment. It was by this treatment that the clay sample used for the experiment was processed.

A. Sample preparation

Four different clay samples were prepared and labeled as follows:

- Sample A: 100g of clay/1400ml of distilled water.
- Sample B: 100g of clay/1400ml of distilled water + 2 wt. % $\text{Na}_2\text{CO}_{3(s)}$
- Sample C: 100g of clay/1400ml of distilled water + 4 wt. % $\text{Na}_2\text{CO}_{3(s)}$
- Sample D: 100g of clay/1400ml of distilled water + 6 wt. % $\text{Na}_2\text{CO}_{3(s)}$

Aim

To determine the viscosities of the clay samples (A-D) at periodic time intervals, and at different speeds of agitation

Procedure

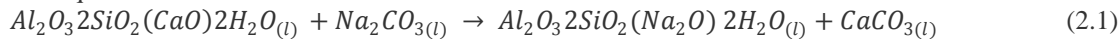
The experiment was conducted at room temperature.



International Journal OF Engineering Sciences & Management Research

Sample A was stirred with the aid of a mechanical agitator by setting the rotor at 300 rpm. The viscometer is washed with distilled water and completely dried. Sample A is then introduced through tube L to slightly above the mark G, using a long pipette to minimize wetting the tube above the mark. The tube is clamped vertically and allowed to stand to maintain equilibrium. The volume of the liquid sample is adjusted so that the meniscus settles at the mark G. It is then sucked through arm N about 5 mm above the mark E. After releasing pressure or suction, the time taken for the bottom of the meniscus to fall from the top edge of mark E to the top edge of mark F is taken at intervals of 5, 10, 15, 20, 25, 30 and 35 sec.

The equation for the reaction is:



The measuring cylinder is then weighed empty. It is then filled with Sample A and weighed. The density, ρ of Sample A is calculated thus:

$$\rho = \frac{m_2 - m_1}{v} \quad (2.2)$$

Where $m_2 = \text{weight of sample A}$

$m_1 = \text{weight of empty cylinder}$
 $v = \text{volume of Sample A}$

The viscosity in Pa.s (Paschal second) is then calculated thus:

$$\mu = K\rho t \quad (2.3)$$

Where

$t = \text{time in seconds for meniscus to fall from E to F}$

$\rho = \text{density of Sample A}$

$K = \text{constant of the instrument as determined by length, } l \text{ travelled between E and F at time, } t.$

This was repeated for speed of agitation of 600 rpm and 900 rpm.

The above procedure was repeated for Samples B, C and D.

Methods of Analysis

Response Surface Methodology

Response surface methodology (RSM) explores the relationship between several explanatory variables and one or more response variables. It consists of a group of mathematical and statistical techniques used in the development of an adequate functional relationship between a response of interest, y , and a number of associated control (or input) variables denoted by $x_1, x_2 \dots x_k$. The main objective of a response surface methodology is to a response (output variable) which is influenced by several independent variables (input variables).

Both the RegStat command and Anovan command were used in the Analysis of Regression Statistics and the Analysis of Variance. Excerpts of the experimental data were gathered in the required format for the statistical study, and the collated data were used in the analysis to generate the necessary statistical parameters useful in the statistical model development and were studied based on the analysis of the variance of the variables of the variables, the estatic value of the model, the goodness of fit (R^2) and Adj. R^2 values of the model and the t-stat values of the variables. The equation for response surface modeling is given as:

$$\mu = C_0 + C_1X_1 + C_2X_2 + C_3X_3 + C_4X_1X_2 + C_5X_1X_3 + C_6X_2X_3 + C_7X_1^2 + C_8X_2^2 + C_9X_3^2 + \dots (2.4)$$

Where

$\mu = \text{viscosity}$

$C_0 - C_9 = \text{constants}$

$X_1 = \text{time}$

$X_2 = \text{concentration of } Na_2CO_3$

$X_3 = \text{speed of agitation}$

Which reduces to:

$$\mu = C_0 + C_1X_2 + C_2X_3 + C_3X_2X_3 + C_4X_2^2 + C_5X_3^2 \quad (2.5)$$

Surface Plots

The surface plot defines a surface by the z-coordinates of points above a grid in the x-y plane, using a straight line to connect the adjacent points. The mesh and surf functions display surfaces in three dimensions.

- Mesh produces wireframe surfaces that colour only the lines connecting the defining points.
- Surf displays both the connecting lines and the faces of the surface in colour.

To display a function of two variables, $z = f(x, y)$, the following steps are taken.

- Generate X and Y matrices consisting of repeated rows and columns, respectively over the domain of the function.
- Use X and Y to evaluate and draw a graph of the function.

The mesh grid function transforms the domain specified by a single vector or two vectors x and y into matrices X and Y for use in evaluating functions of two variables.

In this work, the mesh grid command was used to discretize the points with the range of the factors and the surf command was used for the surface plot with its contour lines using model obtained from section 2.2.1.

Kinetic Study of the Process Using Data-Driven Models

The following models were used in determining the best fit:

Gaussian model: A Gaussian model is a statistical distribution where observation occur in a continuous domain e.g. time and space. In a Gaussian process, every point in some continuous input space is associated with normally distributed random variable. Gaussian functions are important in statistical modelling because of properties inherited from the normal. For example, if a random process is modelled as a Gaussian process, the distribution of various derived quantities can be obtained explicitly. Such quantities include the average value of the process over a range of time and the error in estimating the average using sample values at a small set of time. Gaussian function is shown by the equation below.

$$f(t) = a \exp\left(-\frac{t-b}{c}\right)^2 \quad (2.6)$$

Where

$$f(t) = \mu = \text{viscosity}; a, b, c = \text{constants and } t = \text{time}$$

Exponential model: An exponential function is of the form:

$$f(t) = a \exp bt \quad (2.7)$$

The input variable t occurs as an exponent hence the name. The exponential model is used to model a relationship in which a constant change in the independent variable gives the same proportional change (i.e. percentage increase or decrease) in the dependent variable.

Exponential power model: An exponential power function simply called Power function is similar to exponential function and of the form:

$$f(t) = a \exp bt^c \quad (2.8)$$

In a power function, the independent variable t is raised to a (constant) power c but in an exponential function, the independent variable is the exponent while the base is the constant.

The data so-obtained from the experiments were used in developing the above models.

New Reverse Engineered Model

This new reversed engineered model creates a physical data model by extracting information from an already existing data sources. In other words, it works on a model to create a data. The method of analysis using the kinetic study of the process using data-driven model showed that Gaussian model appropriately describes the behaviour of clay viscosity. The new engineered model then uses this Gaussian model so-obtained to generate data for further uses.

Therefore using the equation for the Gaussian data-driven model,

$$\mu = a \exp\left(-\frac{t-b}{c}\right)^2 \quad (2.6)$$

Differentiating wrt t

$$\frac{d\mu}{dt} = -\frac{2(t-b)}{c^2} \cdot a \exp\left(-\frac{t-b}{c}\right)^2 \quad (2.9)$$

$$\text{But } \mu = a \exp\left(-\frac{t-b}{c}\right)^2$$

Substituting in eqn. (2.8) above gives

$$\frac{d\mu}{dt} = -\frac{2(t-b)}{c^2} \cdot \mu \quad (2.10)$$

$$\text{Letting } \frac{2}{c^2} = k$$

$$\frac{d\mu}{dt} = k(b-t)\mu \quad (2.11)$$

Thus this is a separable variable.

$$\frac{d\mu}{\mu} = k \cdot dt(b-t) \quad (2.12)$$

On integration within $t = t_0$ and $\mu = \mu_0$

$$\ln\left(\frac{d\mu}{d\mu_0}\right) = kbt - \left(\frac{kt^2}{2}\right) \quad (2.13)$$

Letting $kb = \alpha$ and $\frac{k}{2} = \beta$, eqn. (3.12) becomes

$$\mu = \mu_0 \exp(\alpha t - \beta t^2) \quad (2.14)$$

Eqn. (2.14) is thus the equation for the new engineered model and can be used in solving the viscosity of the clay sample at any given time.

RESULTS AND DISCUSSION

Results presentation

Results of the experimentation

Table 3.1: Results of the experiments on Samples (A- D) at 300rpm

Time(s)	100g (clay)	+ 2wt% Na ₂ CO ₃	+ 4wt% Na ₂ CO ₃	+ 6wt% Na ₂ CO ₃
5	0.246Pa.s	0.290Pa.s	0.133Pa.s	0.042Pa.s
10	0.253	0.273	0.144	0.032
15	0.216	0.246	0.152	0.028
20	0.207	0.238	0.160	0.025
25	0.201	0.212	0.161	0.021
30	0.199	0.126	0.175	0.020
35	0.195	0.111	0.171	0.018

Table 3.2: Results of the experiments on Samples (A- D) at 600 rpm

Time(s)	100g (clay)	+ 2wt% Na ₂ CO ₃	+ 4wt% Na ₂ CO ₃	+ 6wt% Na ₂ CO ₃
5	0.398Pa.s	0.332Pa.s	0.333Pa.s	0.093Pa.s
10	0.388	0.355	0.339	0.091
15	0.378	0.314	0.341	0.087
20	0.373	0.305	0.341	0.087
25	0.341	0.302	0.339	0.087
30	0.332	0.294	0.335	0.087
35	0.330	0.268	0.333	0.086

Table 3.3: Results of the experiments on Samples (A- D) at 900 rpm

Time(s)	100g (clay)	+ 2wt% Na ₂ CO ₃	+ 4wt% Na ₂ CO ₃	+ 6wt% Na ₂ CO ₃
5	0.412Pa.s	0.408Pa.s	0.216Pa.s	0.021Pa.s
10	0.417	0.418	0.210	0.023
15	0.433	0.423	0.183	0.025
20	0.430	0.431	0.179	0.027
25	0.412	0.426	0.153	0.039
30	0.412	0.426	0.153	0.039
35	0.402	0.423	0.137	0.041

Results of the statistical analysis using Response Surface Methodology

Table 3.4:Result of the statistical analysis using Regression Statistics

Variables	C ₀ –C ₉	se	t-stat	P _{val}	F-stat
C	-0.1170	0.086917	-1.3461	0.184	sse = 0.11843
X ₁	-0.0042	0.0034896	-1.2169	0.22903	dfe = 53
X ₂	0.0582	0.028013	2.0785	0.042516	dfv = 9
X ₃	0.0014	0.00018675	7.5718	5.4282e-10	ssv = 1.0053
X ₁ X ₂	6.5536e-04	0.0003647	1.7970	0.078036	f = 49.987
X ₁ X ₃	1.7341e-06	2.4313e-06	0.71325	0.47882	p _{val} = 0
X ₂ X ₃	-8.5119e-05	1.4899e-05	-5.7170	5.0869e-07	
X ₁ ²	-1.5026e-06	6.8768e-05	-0.21851	0.82787	
X ₂ ²	-0.0109	0.0031584	-3.4413	0.0011369	
X ₃ ²	-8.1323e-07	1.4037e-07	-5.7934	3.8527e-07	
	R ² =0.8946	Adj.R ² =0.8767	mse=0.0022		

Table 3.5:Result of the statistical analysis using Analysis of Variance

Source	Sum of sq.	d.f	Mean sq.	F	Prob.>F
X1	0.00914	6	0.00152	0.4	0.8778
X2	0.77366	2	0.38683	100.76	0
X3	0.14124	2	0.07062	18.39	0
Error	0.19964	52	0.00384		
Total	1.12368	62			

Surface Response Plots

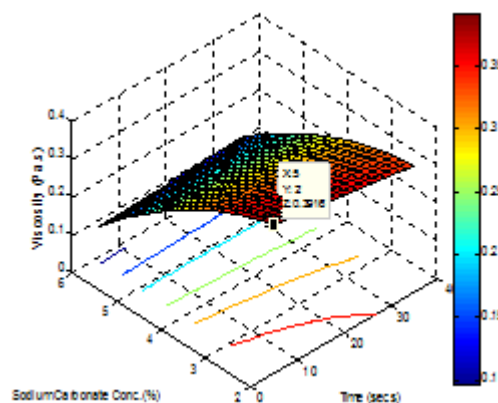


Fig3.1: Surface plot of viscosity versus time and sodium carbonate concentration

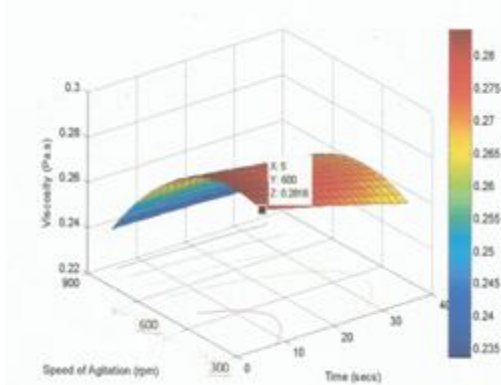


Fig 3.2: Surface plot of viscosity versus time and speed of agitation

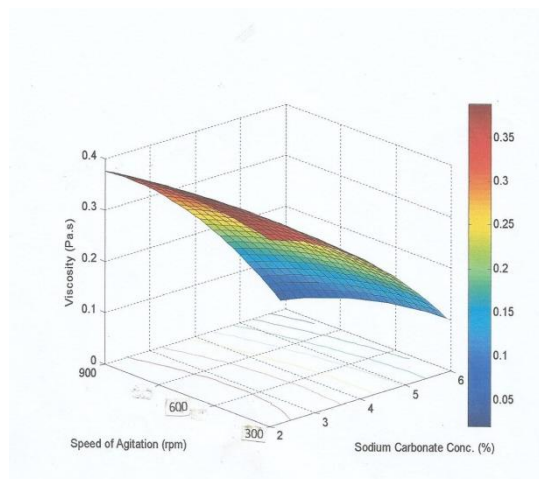


Fig3.3: Surface plot of viscosity versus Sodium carbonate conc. and speed of agitation

Results of the analysis of the kinetic study of the process using data-driven models

Using the equations (2.6 – 2.8) and solving for the constants, the following graphs and tables were obtained.

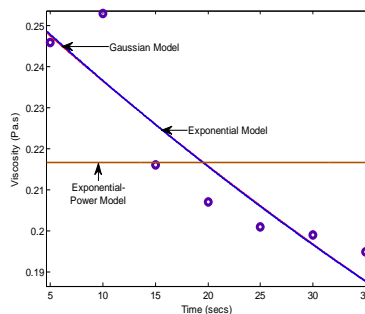


Figure 3.4: Graph of data-driven model for control sample at 300rpm

Table 3.6: Numerical fit data for data-driven model for control sample at 300rpm

Model	a	b	c	R ²	AdjR ²
Gaussian	15.48	-907.2	448.6	0.8382	0.7573
Exponential	0.2597	-0.0093	-	0.8399	0.8079
Exponential power	0.2166	0.0036	1.16e-5	-4.86e-8	-0.5

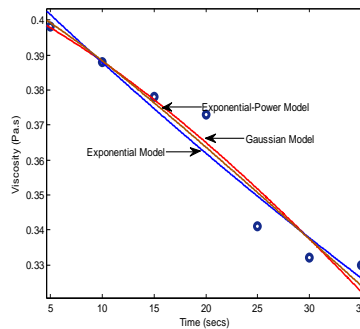


Figure 3.5: Graph of data-driven model for control sample at 600rpm

Table 3.7: Numerical fit data for data-driven model for control sample at 600rpm

Model	a	b	c	R ²	AdjR ²
Gaussian	0.4217	-21.14	108.3	0.9433	0.9150
Exponential	0.4158	-0.0069	-	0.9432	0.9119
Exponential power	0.4073	-0.0026	1.256	0.9474	0.9211

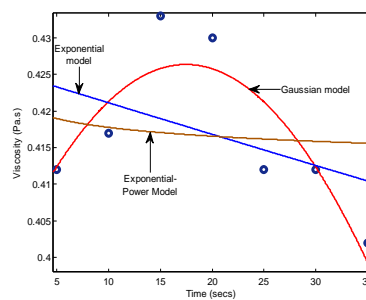


Figure 3.6: Graph of data-driven model for control sample at 900rpm

Table 3.8: Numerical fit data for data-driven model for control sample at 900rpm

Model	a	b	c	R ²	AdjR ²
Gaussian	0.4264	17.5	68.32	0.7503	0.6254
Exponential	0.4255	-0.0010	-	0.1805	0.0166
Exponential power	0.0927	1.515	-0.0028	0.0330	-0.451

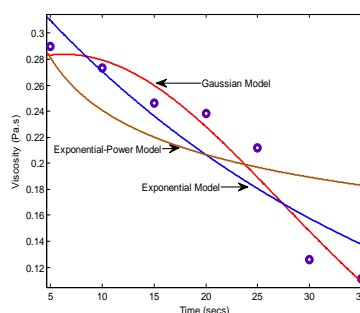


Figure 3.7: Graph of data-driven model for 2wt. % Na₂CO₃ at 300 rpm

Table 3.9: Numerical fit data for data-driven model for 2wt. % Na₂CO₃ at 300 rpm

Model	a	b	c	R ²	AdjR ²
Gaussian	0.2838	6.367	29.26	0.9528	0.9291
Exponential	0.3551	-0.027	-	0.8566	0.8280
Exponential power	5.20e-5	8.97	-0.0264	0.5834	0.3751

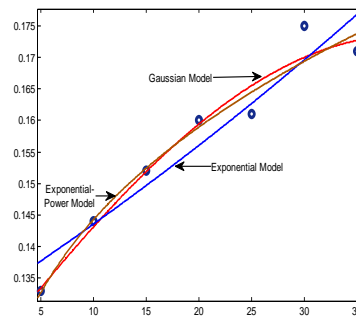


Figure 3.8: Graph of data-driven model for 4wt.% Na_2CO_3 at 300 rpm

Table 3.10 Numerical fit data for data-driven model for 4wt. % Na_2CO_3 at 300 rpm

Model	a	b	c	R^2	Adj R^2
Gaussian	0.1735	39.77	67.83	0.9622	0.9433
Exponential	0.1321	0.0083	-	0.9169	0.9002
Exponential power	0.0787	0.3705	0.2134	0.9597	0.9395

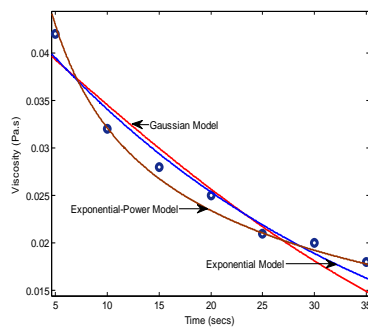


Figure 3.9: Graph of data-driven model for 6wt.% Na_2CO_3 at 300 rpm

Table 3.11: Numerical fit data for data-driven model for 6wt. % Na_2CO_3 at 300 rpm

Model	a	b	c	R^2	Adj R^2
Gaussian	0.0697	-41.8	61.89	0.9245	0.8867
Exponential	0.0458	-0.029	-	0.9580	0.9496
Exponential power	1.263	-2.789	0.1192	0.9869	0.9804

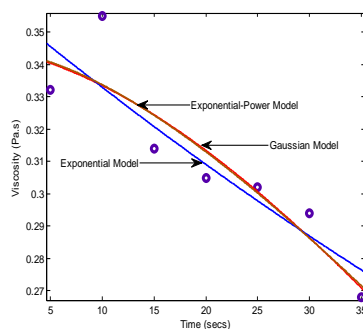


Figure 3.10: Graph of data-driven model for 2wt.% Na_2CO_3 at 600 rpm

Table 3.12 Numerical fit data for data-driven model for 2wt. % Na₂CO₃ at 600 rpm

Model	a	b	c	R ²	AdjR ²
Gaussian	0.3474	-7.007	84.24	0.8315	0.7472
Exponential	0.3588	-0.007	-	0.8518	0.7742
Exponential power	0.3442	-0.001	1.635	0.8331	0.7497

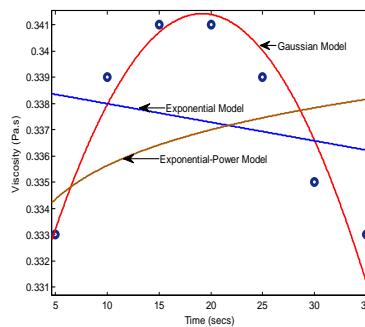


Figure 3.11: Graph of data-driven model for 4wt. % Na₂CO₃ at 600 rpm

Table 3.13: Numerical fit data for data-driven model for 4wt. % Na₂CO₃ at 600 rpm

Model	a	b	c	R ²	Adj R ²
Gaussian	0.3414	19.18	90.66	0.8903	0.8354
Exponential	0.3387	-0.0002	-	0.0470	-0.144
Exponential power	0.3116	0.0622	0.0769	-0.1564	-0.735

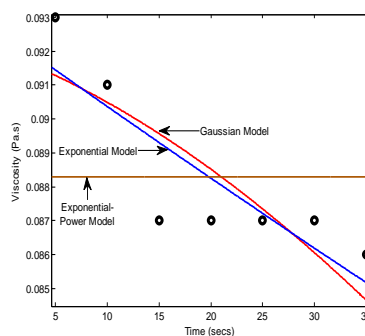


Figure 3.12: Graph of data-driven model for 6wt. % Na₂CO₃ at 600 rpm

Table 3.14 Numerical fit data for data-driven model for 6wt. % Na₂CO₃ at 600 rpm

Model	a	b	c	R ²	AdjR ²
Gaussian	0.0932	-20.51	179.5	0.6389	0.4583
Exponential	0.0926	-0.0023	-	0.7324	0.6788
Exponential power	0.0883	6.7e-5	10.0e-5	-4.33e-7	-0.5

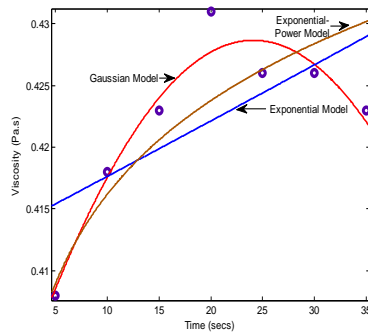


Figure 3.13: Graph of data-driven model for 2wt.% Na₂CO₃ at 900 rpm

Table 3.15 Numerical fit data for data-driven model for 2wt.% Na₂CO₃ at 900 rpm

Model	a	b	c	R ²	AdjR ²
Gaussian	0.4287	24.13	87.05	0.9370	0.9054
Exponential	0.4132	-0.001	-	0.4432	0.3318
Exponential power	0.2218	0.5726	0.0410	0.6336	0.4504

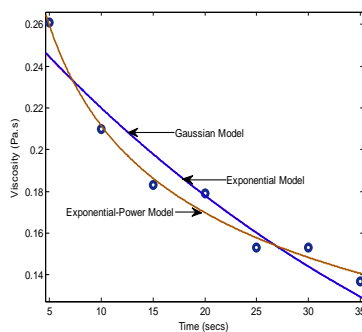


Figure 3.14: Graph of data-driven model for 4wt.% Na₂CO₃ at 900 rpm

Table 3.16: Numerical fit data for data-driven model for 4wt.% Na₂CO₃ at 900 rpm

Model	a	b	c	R ²	AdjR ²
Gaussian	7.72e7	-1856	420.7	0.9265	0.8898
Exponential	0.2723	-0.021	-	0.9275	0.9130
Exponential power	5.164	-2.561	0.0960	0.9854	0.9781

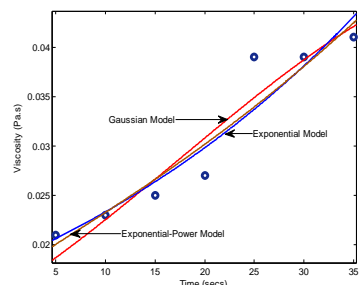


Figure 3.15: Graph of data-driven model for 6wt.% Na₂CO₃ at 900 rpm

Table 3.17 Numerical fit data for data-driven model for 6wt.% Na₂CO₃ at 900 rpm

Model	a	b	c	R ²	AdjR ²
Gaussian	0.0479	52.52	48.98	0.9081	0.8621
Exponential	0.0182	0.0246	-	0.9026	0.8831
Exponential power	0.0163	0.0575	0.7912	0.9052	0.8577

Results of the analysis of the new engineered model

Solving equation 2.14 using the data from the experiments, the following graphs and tables were obtained.

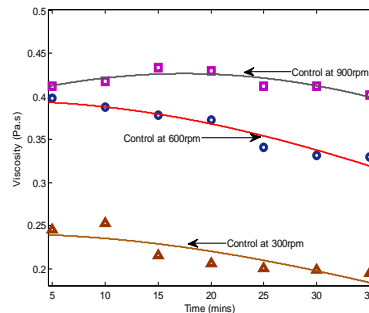


Figure 3.16: Graph of new reverse engineered model for control sample

Table 3.18: Numerical fit data for new reverse engineered model for control sample

Speed (rpm)	α	β	μ_0	R^2	AdjR ²
300	2.31e-14	0.00017	0.2407	0.7255	0.6707
600	2.13e-12	0.00017	0.3946	0.9209	0.9050
900	0.0075	0.00021	0.3993	0.7503	0.6254

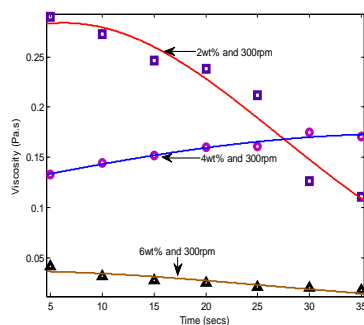


Figure 3.17: Graph of new reverse engineered model at 300rpm

Table 3.19: Numerical fit data for new reverse engineered model at 300 rpm

wt. %	α	β	μ_0	R^2	AdjR ²
2	0.0148	0.00116	0.2707	0.9528	0.9291
4	0.0173	0.00022	0.1231	0.9622	0.9433
6	2.22e-4	0.00076	0.0370	0.8380	0.7981

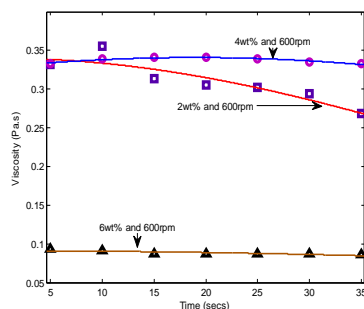


Figure 3.18: Graph of new reverse engineered model at 600rpm

Table 3.20: Numerical fit data for new reverse engineered model at 600rpm

wt. %	α	β	μ_0	R^2	Adj R^2
2	0.0064	0.00013	0.3969	0.9570	0.9097
4	2.75e-14	0.00051	0.2305	0.9518	0.9048
6	0.03991	0.00035	0.0159	0.9102	0.8653

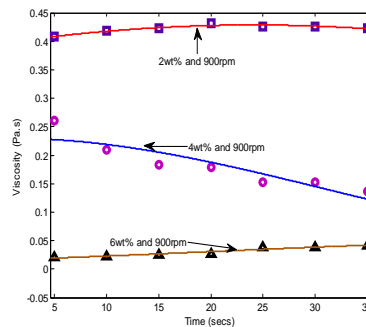


Figure 3.19: Graph of new reverse engineered model at 900rpm

Table 3.21: Numerical fit data for new reverse engineered model at 900rpm

wt. %	α	β	μ_0	R^2	Adj R^2
2	6.21e-8	0.0002	0.3400	0.8279	0.7934
4	0.0040	0.0001	0.3282	0.9128	0.8692
6	2.72e-5	5.94e-5	0.0909	0.5410	0.3115

Discussion of Result

Using the result of the experiments in Tables (3.1 - 3.3) and the equation for response surface modeling,

$$\mu = C_0 + C_1X_1 + C_2X_2 + C_3X_3 + C_4X_1X_2 + C_5X_1X_3 + C_6X_2X_3 + C_7X_1^2 + C_8X_2^2 + C_9X_3^2 +.. \quad (2.3)$$

Where

$\mu = \text{viscosity}$

$C_1 - C_9 = \text{constants}$

$X_1 = \text{time}$

$X_2 = \text{concentration of } Na_2CO_3$

$X_3 = \text{speed of agitation}$

The result of the MATLAB programming of the response surface modeling for solving Eqn. 2.3 is shown in Table 3.4.

Using a confidence interval of 95% and significance of $|t\text{-start}| \geq 2$ and $p_{val} \leq 0.05$,

Eqn. 2.3 reduces to

$$\mu = C_0 + C_1X_2 + C_2X_3 + C_3X_2X_3 + C_4X_2^2 + C_5X_3^2 \quad (2.4)$$

From Table 3.4 it can be deduced that time (X_1) is the least significant of the variables while concentration and speed of agitation are significant variables. Removing terms containing X_1 from Eqn. 2.3 reduced the model to Eqn. 2.4.

The R^2 value reveals that the statistical model explains about 89% of the observed variability in the experimental data. This is a measure of the model accuracy. The F-statistical p-value is zero. Thus the model is adequate since the value is <0.05 . The mean square error (mse) value is expected to be close to zero and the fit has a value of 0.0022 which is acceptable.

The t-stat value (which should be a magnitude of 2 or more) and its p-value (which should be ≤ 0.05 at 95% confidence) reveals that concentration of Na_2CO_3 , speed of agitation, interaction between concentration of Na_2CO_3 and speed of agitation and the quadratic terms of concentration of Na_2CO_3 and speed of agitation are the significant terms. Interaction between time and concentration of Na_2CO_3 is only significant at 90% confidence interval.

International Journal OF Engineering Sciences & Management Research

The Analysis of variance table, Table 3.5 based on prob. > F-value reveals that concentration of Na_2CO_3 and speed of agitation are the significant variables, since they have values ≤ 0.05 . Time is not a significant variable. This corroborates the observation from the t-stat values of Table 4.4 that time is not significant.

From Fig 3.1, the surface plot shows a progressive change in the colour gradient as the concentration of sodium carbonate increases while there is very little change in the colour gradient as time increases. This means that time is insignificant.

In addition, viscosity has a somewhat quadratic relationship with Na_2CO_3 concentration but a linear relationship with time as can be seen by the profile of the plot. The contour lines are not all parallel to each other. This indicates that the interaction between time and Na_2CO_3 concentration may be significant. Thus, though time may not be significant as a variable, its interaction with Na_2CO_3 concentration shows some significance at 90% confidence as can be seen from the t-stat and p-value.

From Fig 3.2, the surface plot shows a progressive change in the colour gradient as the speed of agitation increases while there is very little change in the colour gradient as time increases. This means that time is insignificant.

In addition, viscosity has a somewhat quadratic relationship with speed of agitation but a linear relationship with time as can be seen by the profile of the plot. The contour lines are not all parallel to each other. This indicates that the interaction between time and speed of agitation may be significant.

Thus, though time may not be significant as a variable, its interaction with speed of agitation shows some significance at 90% confidence as can be seen from the t-stat and p-value.

From Fig 3.3, the surface plot shows greater change in the colour gradients as speed of agitation increases and no change as sodium carbonate concentration increases.

In addition, viscosity has a somewhat quadratic relationship with both Na_2CO_3 concentration and speed of agitation as can be seen by the profile of the plots. The not-too-parallel nature of the contour lines indicates that the parameters are significant both as variables and in interaction. This clearly agrees with the t-stat and p-values.

Therefore, both speed of agitation and concentration of sodium carbonate are significant both as variables and in interaction in the analysis of viscosity of clay while time is the least significant as a variable but may be significant in interaction with both Na_2CO_3 concentration and speed of agitation.

From Table 3.6, the R^2 of the Exponential model is 0.8399 as against 0.8382 and -4.826×10^{-8} for Gaussian model and Exponential power model respectively. This showed that the Exponential model describes the behaviour of the viscosity of the clay sample for control at 300rpm. Similarly, the Exponential model has the line of best fit as shown in Fig. 3.4.

From Table 3.7, the R^2 of the Exponential power model is 0.9474 as against 0.9433 and 0.9432 for Gaussian model and Exponential model respectively. This showed that the Exponential power describes the behaviour of the viscosity of the clay sample for control at 600rpm. Similarly, the Exponential power model has the line of best fit as shown in Fig. 3.5.

From Table 3.8, the R^2 of the Gaussian model is 0.7503 as against 0.1805 and 0.03295 for Exponential model and Exponential power model respectively. This showed that the Gaussian model describes the behaviour of the viscosity of the clay sample for control at 900rpm. Similarly, the Gaussian model has the line of best fit as shown in Fig.3.6.

From Table 3.9, the R^2 of the Gaussian model is 0.9528 as against 0.8566 and 0.5834 for Exponential model and Exponential power model respectively. This showed that the Gaussian model describes the behaviour of the viscosity of the clay sample at 2 wt. % and 300rpm. Similarly, the Gaussian model has the line of best fit as shown in Fig. 3.7.



International Journal OF Engineering Sciences & Management Research

From Table 3.10, the R^2 of the Gaussian model is 0.9622 as against 0.9169 and 0.9597 for Exponential model and Exponential power model respectively. This showed that the Gaussian model describes the behaviour of the viscosity of the clay sample at 4wt. % and 300rpm. Similarly, the Gaussian model has the line of best fit as shown in Fig. 3.8.

From Table 3.11, the R^2 of the Exponential power model is 0.9869 as against 0.9245 and 0.9580 for Gaussian model and Exponential model respectively. This showed that the Exponential power model describes the behaviour of the viscosity of the clay sample at 6wt. % and 300rpm. Similarly, the Exponential power model has the line of best fit as shown in Fig. 3.9.

From Table 3.12, the R^2 of the Exponential model is 0.8518 as against 0.8315 and 0.8331 for Gaussian model and Exponential power model respectively. This showed that the Exponential model describes the behaviour of the viscosity of the clay sample at 2wt. % and 600rpm. Similarly, the Exponential model has the line of best fit as shown in Fig. 3.10.

From Table 3.13, the R^2 of the Gaussian model is 0.8903 as against -0.04698 and -0.1564 for Exponential model and Exponential power model respectively. This showed that the Gaussian model describes the behaviour of the viscosity of the clay sample at 4wt. % and 600rpm. Similarly, the Gaussian model has the line of best fit as shown in Fig. 3.11.

From Table 3.14, the R^2 of the Exponential model is 0.7324 as against 0.6389 and -0.4334e-07 for Gaussian model and Exponential power model respectively. This showed that the Exponential model describes the behaviour of the viscosity of the clay sample at 6wt. % and 600rpm. Similarly, the Exponential model has the line of best fit as shown in Fig. 3.12.

From Table 3.15, the R^2 of the Gaussian model is 0.9370 as against 0.4432 and 0.6336 for Exponential model and Exponential power model respectively. This showed that the Gaussian model describes the behaviour of the viscosity of the clay sample at 2wt. % and 900rpm. Similarly, the Gaussian model has the line of best fit as shown in Fig. 3.13.

From Table 3.16, the R^2 of the Exponential power model is 0.9854 as against 0.9265 and 0.9275 for Gaussian model and Exponential model respectively. This showed that the Exponential power model describes the behaviour of the viscosity of the clay sample at 4wt. % and 900rpm. Similarly, the Exponential model has the line of best fit as shown in Fig. 3.14.

From Table 3.17, the R^2 of the Gaussian model is 0.9081 as against 0.9026 and 0.9052 for Exponential model and Exponential power model respectively. This showed that the Gaussian model describes the behaviour of the viscosity of the clay sample at 6wt. % and 900rpm. Similarly, the Gaussian model has the line of best fit as shown in Fig. 3.15.

The Gaussian model, in addition to having the higher values of R^2 (50% of the total R^2 compared to 25% each for Exponential model and Exponential power model) and the lines of best fit, has 57.14% of the total R^2 that fall with confidence intervals of 90% and above as against 42.86% for Exponential power model and 0% for Exponential model.

Hence Gaussian model describes the viscosity of the clay samples in relation to time, concentration of sodium carbonate and speed of agitation.

Solving equation for Gaussian model, Eqn. 2.6 further gives rise to Eqn. 2.14

Hence Eqn. 2.14 is therefore the relationship between the initial viscosity, μ_0 and time, t to viscosity, μ at any given time. This process consists of a forward and reverse reaction. The reaction is first order with respect to time while the reverse reaction is second order with respect to time. α and β are forms of rate constants for the forward and reverse reactions respectively and may be functions of speed of agitation and treatment concentration.

$$\mu = \mu_0 \exp(\alpha t - \beta t^2) \quad (3.14)$$

Solving for μ_0 , α and β gives rise to Tables (3.18 – 3.21) and graphs of Fig. (4.16 – 4.19) at the various speeds of agitation.



International Journal OF Engineering Sciences & Management Research

From Table 3.18, result is poor for the new reverse engineered model for the control at various rpm as none of the $R^2 \geq 0.95$. This is illustrated by Fig 3.16. Comparing this result with those with various concentration of sodium carbonate shows that sodium carbonate actually modifies the viscosity of the clay sample.

From Table 3.19, the new reverse engineered model at 300 rpm, the R^2 of 2 wt. % and 4 wt. % are 0.9528 and 0.9622 respectively as against the R^2 of 6 wt. % of 0.8380. This is illustrated by Fig. 3.17. Hence the experiment gives a very good result at 300 rpm.

From Table 3.20, the new reverse engineered model at 600 rpm, the R^2 at 2 wt. %, 4 wt. % and 6 wt. % are 0.9570, 0.9518 and 0.9102 respectively. This is illustrated by Fig. 3.18. Hence the experiment gives a very good result at 600 rpm.

From Table 3.21, the new reverse engineered model at 900 rpm, the R^2 at 2 wt. %, 4 wt. % and 6 wt. % are 0.8279, 0.9126 and 0.5410 respectively. This is illustrated by Fig. 3.19. Hence the experiment gives a poor result at 900 rpm with none of the $R^2 \geq 0.95$.

CONCLUSION

The research was focused on the enhancement of the performance of Ubakala clay sample for use as drilling mud. A sample of Nigerian clay (Ubakala clay) was used for the research. The clay sample was collected in a raw state, processed and experiments conducted on viscosity which is a very important property of drilling mud. Various concentrations of sodium carbonate were mixed with the clay sample and experiments were conducted to determine the viscosities of the control and the clay-sodium carbonate mixture at periodic time intervals and various speeds of agitation. Response Surface Methodology was used, and with the aid of a MATLAB programming, to study the data obtained from the experiment. The results showed that sodium carbonate concentration, speed of agitation and their various interactions terms and quadratic terms are the significant variables in the statistical model with time being the least significant of the three factors studied. Furthermore, on analysis of the kinetics of the process, a Gaussian model, having the highest values of R^2 (50% for Gaussian model, and 25% each for Exponential and Exponential Power models) and the lines of best fit, effectively describes the kinetics of the process and the viscosity of the clay samples in relation to time, concentration of sodium carbonate and speed of agitation. Further work on the Gaussian model gave rise to a new model that can be used to determine the values of the kinetic constants. This new model showed that a speed of agitation between 300rpm and 600rpm gave the best result for the process

REFERENCES

1. Adam T.B. Jr, Chenevert M.E., Millheim K.K. and Young Jr F.S. (1986). *Applied Drilling Drilling Fluids (Vol. 2)*. (J. F. S.P, Ed.) Texas: SPE Textbook Series, Richardson.
2. Amorim V.L., Gomes C.M., Lira H. L., Franca, K. B. and Ferreira H. C. (2007). *Bentonites from Boa Vista, Brazil: Physical, Mineralogical and Rheological Properties. Research Materials*. (7 ed., Vol. 4).
3. Amos G. (2011). *MATLAB: An Introduction with Applications (4 ed.)*. New York: John Wiley and Sons Inc.
4. Andre´ I. K. and Siuli M. (2010). *Response Surface Methodology. (Vol. 2)*. New York: John Wiley & Sons, Inc.
5. Ben B., Neal D., Brad S., Louise B., Lindsay, F. and Mike, H. (1994). *Designing and Managing Drilling Fluids*. Retrieved from [http://www.slb.com/media/File/resources/oilfield_](http://www.slb.com/media/File/resources/oilfield_review/ors94/0494/p33_43.ashx)
6. [review/ors94/0494/p33_43.ashx](http://www.slb.com/media/File/resources/oilfield_review/ors94/0494/p33_43.ashx)
7. Clark R.K. and Nahm J. J. (1980). *Drilling Fluids. In Encyclopedia of Chemical Technology (2 ed., Vol. 17, pp. 143-165)*. New York: John Wiley and Sons Ltd.
8. Emofurieta W. (2010). *International Conference on 'Modern Mining Processing'*. Abuja. Retrieved from <http://www.nigerianewsdirect.com>
9. Ezeribe I.E. and Oyedeji O.A. (2005). *The suitability of Nigerian bentonites and black cotton soils as drilling mud. Nigerian Geological Survey Agency, 2B*.
10. Falode O.A., Ehinola O.A. and Nebeife P.C. (2007). *Evaluation of Local Bentonitic Clay as Oil Well Drilling Fluids in Nigeria. Applied Clay Science, 39, 19-27*. Retrieved from <http://www.sciencedirect.com>
11. Jackson N.L. (1957). *Frequency Distribution of Clay Minerals in Major Great Soil Groups as Related to Factors of Soil Formation. Clay Minerals, 5, 279-288*.



International Journal OF Engineering Sciences & Management Research

12. Nestle, C.A. (1944, *Engineering and Science Monthly*, August-September, 2011). *Mud Engineering. British Journal of Applied Science and Technology*, 1(4), 13-16.
13. Nweke O.M., Igwe E.O. and Nnabo P.N. (2015). *Comparative Evaluation of Clays from Abakaliki Formation with Commercial Bentonite Clays for Use as Drilling Mud. African Journal of Environmental Science and Technology*. Retrieved from <http://www.academicjournals.org>
14. Omole O., Malomo S. and Akande S. (1989). *The Suitability of Nigerian Black Soil Clay as Drilling Mud Clays. Applied Clay Science*, 4, 357-372.
15. Parkes W.R. (1982). *Occupational Lung Disorders*. London: Butterworths.
16. Preston L.M. (1974). *Drilling Practices Manual*. Oklahoma, USA: The Petroleum Publishing Co.
17. Uba H.D. (1988). *Hydrothermal Reactions of Wyoming Bentonite in The Presence of Mixed Salts and Their Effects on the Rheology of Bentonite Fluids*. M.Sc. Thesis, Texas Technical University, Graduate Faculty, Texas.